γ-Aminobutyric Acid Type A Receptor Modulation by Etomidate Analogs

Ervin Pejo, B.S., Peter Santer, M.D., Lei Wang, Ph.D., Philip Dershwitz, B.S., S. Shaukat Husain, D.Phil., Douglas E. Raines, M.D.

ABSTRACT

Background: Etomidate is a highly potent anesthetic agent that is believed to produce hypnosis by enhancing γ-aminobutyric acid type A ($GABA_A$) receptor function. The authors characterized the $GABA_A$ receptor and hypnotic potencies of etomidate analogs. The authors then used computational techniques to build statistical and graphical models that relate the potencies of these etomidate analogs to their structures to identify the specific molecular determinants of potency.

Methods: $GABA_A$ receptor potencies were defined with voltage clamp electrophysiology using $\alpha_1\beta_3\gamma_2$ receptors harboring a channel mutation (α_1[L264T]) that enhances anesthetic sensitivity (n = 36 to 60 measurements per concentration–response curve). The hypnotic potencies of etomidate analogs were defined using a loss of righting reflexes assay in Sprague Dawley rats (n = 9 to 21 measurements per dose–response curve). Three-dimensional quantitative structure–activity relationships were determined *in silico* using comparative molecular field analysis.

Results: The $GABA_A$ receptor and hypnotic potencies of etomidate and the etomidate analogs ranged by 91- and 53-fold, respectively. These potency measurements were significantly correlated (r^2 = 0.72), but neither measurement correlated with drug hydrophobicity (r^2 = 0.019 and 0.005, respectively). Statistically significant and predictive comparative molecular field analysis models were generated, and a pharmacophore model was built that revealed both the structural elements in etomidate analogs associated with high potency and the interactions that these elements make with the etomidate-binding site.

Conclusions: There are multiple specific structural elements in etomidate and etomidate analogs that mediate $GABA_A$ receptor modulation. Modifying any one element can alter receptor potency by an order of magnitude or more. **(ANESTHESIOLOGY 2016; 124:651-63)**

ETOMIDATE is a highly selective intravenous anesthetic agent that is widely believed to produce hypnosis by binding to a site (or class of sites) on the γ-aminobutyric acid type A ($GABA_A$) receptor.[1–5] Although structural information regarding this site is quite limited, there is growing evidence that it is located at the interface between the $GABA_A$ receptor's α and β subunits in the transmembrane domain.[6–8] The result of such binding is an enhancement of $GABA_A$ receptor function.[9,10] Specifically, etomidate binding increases agonist potency for activating (*i.e.*, opening) $GABA_A$ receptors, a process termed "agonist potentiation." In the absence of agonist, etomidate binding also directly activates $GABA_A$ receptors. Although the agonist potentiating and direct activating actions are measurable using electrophysiologic techniques over distinct etomidate concentration ranges (low and high, respectively), it has been proposed that the underlying receptor mechanism for these two enhancing actions is the same (stabilizing the open channel state) and that they reflect etomidate binding to the same receptor site(s).[10–12] In addition to enhancing $GABA_A$ receptor function, etomidate, etomidate analogs, and other anesthetics can inhibit the receptor's function.[13–15] This inhibitory action typically occurs only at very high anesthetic concentrations and is likely mediated by a site that is distinct from that which produces enhancement.

What We Already Know about This Topic

- Considerable evidence indicates that the intravenous anesthetic etomidate produces hypnosis by enhancing γ-aminobutyric acid type A receptor function
- Structural information regarding the binding site suggests that it is located at the transmembrane interface between the α and β subunits

What This Article Tells Us That Is New

- By using both *in vitro* and *in vivo* assays of etomidate action, γ-aminobutyric acid type A receptor and hypnotic potencies of etomidate and 22 etomidate analogs were significantly correlated, supporting a direct role for receptor activation in etomidate-induced hypnosis
- Molecular modeling computational techniques were used to build pharmacophore models that revealed multiple structural elements associated with high-potency binding-site interactions of etomidate

Studies of etomidate's two enantiomers indicate that the structural requirements for $GABA_A$ receptor binding and enhancement can be quite specific. Although etomidate's enantiomers have identical physical properties, they differ

Submitted for publication May 28, 2015. Accepted for publication November 20, 2015. From the Department of Anesthesia, Critical Care, and Pain Medicine, Massachusetts General Hospital, Boston, Massachusetts (E.P., P.S., P.D., S.S.H., D.E.R.); and Certara L.P., St. Louis, Missouri (L.W.).

 Anesthesiology 2016; 124:651-63

<zdoi;10.1097/ALN.0000000000000992>

by 1 to 2 orders of magnitude in their *in vitro* affinities and potencies for the $GABA_A$ receptor and, consequently, their *in vivo* hypnotic potencies.[3,13,16] Other small structural modifications around the chiral center similarly impact $GABA_A$ receptor and hypnotic potencies, implying that this region of etomidate's molecular scaffold is a critical determinant of pharmacologic activity.[13] The pharmacologic importance of other regions is unknown.

Over the past several years, our laboratory has developed multiple novel etomidate analogs that contain structural modifications in various parts of etomidate's molecular scaffold and exhibit unique pharmacology.[13,17–20] These compounds include etomidate esters that are ultrarapidly metabolized, pyrrole analogs devoid of adrenocortical side effects, and achiral analogs with reduced hypnotic and adrenocortical inhibitory potencies. Although it seems likely that only a handful of these analogs have potential value as clinical anesthetic agents, together they can be used as pharmacologic tools for structure–activity relationship studies to better define the structural determinants of etomidate's enhancing action on the $GABA_A$ receptor. Such information may also provide clues regarding the nature of the etomidate-binding site and ultimately suggest ways of making more potent analogs.

In this study, we quantified the potencies with which etomidate analogs directly activate the heteromeric $GABA_A$ receptors. We incorporated a channel mutation into the receptor that stabilizes its open state, thus increasing anesthetic sensitivity and allowing more complete anesthetic concentration–response curves to be generated (1) before reaching aqueous saturation at high anesthetic concentrations and (2) without the potentially confounding effects of a coadministered agonist.[10,13,21] We also defined the potencies with which etomidate analogs produce hypnosis in rats. We then used computational techniques to build statistical and graphical models that relate the $GABA_A$ receptor and hypnotic potencies of these etomidate analogs to their physical structures (*i.e.*, steric and electrostatic properties) in a three-dimensional space.

Materials and Methods

Animals

All studies were conducted with the approval of and in accordance with the regulations of the Institutional Animal Care and Use Committee at Massachusetts General Hospital (Boston, MA). *Xenopus laevis* adult female frogs were purchased from Xenopus One (USA). Adult male Sprague-Dawley rats (300 to 450 g) were purchased from Charles River Laboratories (USA).

Etomidate and Etomidate Analogs

Figures 1 and 2 show the structures of etomidate and the etomidate analogs used in this study and indicate their names and compound numbers (1 to 23). The structures of etomidate and metomidate are shown in the top row of figure 1. Etomidate was purchased from Bachem Americas (USA), and metomidate was synthesized by Aberjona Laboratories (USA) using the general approach previously reported for etomidate.[22] The second row in figure 1 shows the structures of S-etomidate, dihydrogen etomidate, and cyclopropyl etomidate. These etomidate analogs, which have chiral center modifications, were synthesized as previously described.[13] The third row in figure 1 shows the structures of the pyrrole etomidate analogs carboetomidate and 4-pyridine carboetomidate. Both compounds were synthesized by Aberjona Laboratories. The last row in figure 1 shows the structures of racemic pentafluoroetomidate, S-pentafluoroetomidate, and R-pentafluoroetomidate. The first two compounds were synthesized by Aberjona Laboratories using the approach previously reported for etomidate using racemic 1-pentafluorphenylethanol or R-1-pentafluorphenylethanol, respectively, in the place of 1-phenylethanol.[22] R-pentafluoroetomidate was not synthesized because the necessary chiral alcohol reagent (S-1-pentafluorphenyl ethanol) was not commercially available. However, potency values for this enantiomer were estimated from those determined for racemic pentafluoroetomidate and S-pentafluoroetomidate. The structures of the etomidate esters used in this study are shown in figure 2. They were synthesized as previously described.[17,19]

$GABA_A$ Receptor Electrophysiology

Oocytes were harvested from frogs and injected with mRNA encoding the α_1(L264T), β_3, and γ_2 subunits of the human $GABA_A$ receptor (5 ng of mRNA total at a subunit ratio of 1:1:3). After RNA injection, oocytes were incubated in ND96 buffer (96 mM NaCl, 2 mM KCl, 1.8 mM $CaCl_2$, 1 mM $MgCl_2$, 5 mM HEPES, pH = 7.4) containing 0.1 mg/ml ciprofloxacin and 0.05 mg/ml gentamicin for 18 to 48 h at 18°C before electrophysiologic study. Electrophysiologic recordings were performed at room temperature using the whole cell two-electrode voltage clamp technique as described previously.[20] In each experiment, the peak amplitude was defined as the difference between the baseline current before etomidate analog infusion and the single highest point in the current trace during infusion. This amplitude was then normalized to the peak amplitude measured in control currents elicited by 100 μM GABA (a concentration of GABA that maximally activates $GABA_A$ receptors) in the same oocyte. For each etomidate analog, the concentration–mean response data were fit to a Hill equation with minima and maxima constrained to 0 and 100%, respectively, using equation 1 as previously described[13]:

$$\text{Normalized peak amplitude} = 100 / \left(1 + \left(\frac{EC_{50}}{[\text{Analog}]}\right)^n\right)$$

where EC_{50} is the etomidate analog concentration that evokes a peak current amplitude that is half that evoked by 100 μM GABA, [Analog] is the etomidate analog concentration, and n is the Hill coefficient.

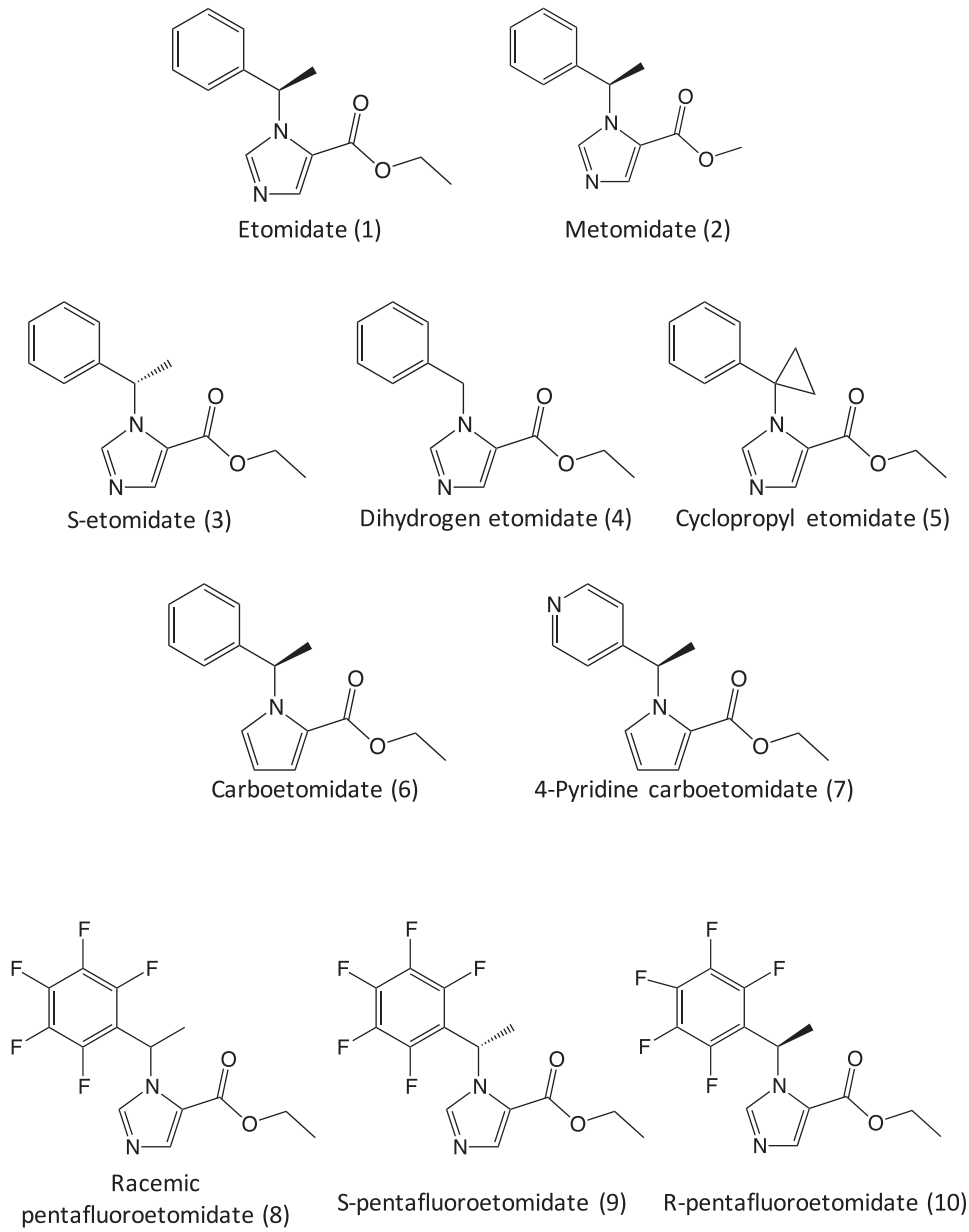

Fig. 1. Chemical structures of etomidate analogs, their names, and their numerical designations. *Top row* shows the parent compounds etomidate and metomidate. *Second row* compounds are etomidate analogs with modifications around the chiral center. *Third row* compounds are pyrrole etomidate analogs. *Fourth row* compounds are fluorinated etomidate analogs.

Rat Loss of Righting Reflexes Assay

The hypnotic potencies of etomidate analogs were assessed in rats using a loss of righting reflexes (LORR) assay.[17] In brief, the desired dose of analog in dimethyl sulfoxide vehicle (0.1 to 0.3 ml) was rapidly injected through an intravenous catheter placed in a tail vein followed by a normal saline flush. Immediately afterward, rats were turned supine. A rat was judged to have LORR if it failed to turn itself back onto all four paws within 5 s after drug administration. For each analog, the median effective dose (ED_{50}) for LORR was determined from a data set of at least 24 separate doses using the method of Waud.[23] For *in silico* modeling studies, each ED_{50} value expressed in milligram per kilogram was converted to units of micromolar per kilogram using the analog's molecular weight.

Determination of Octanol:Water Partition Coefficients

The octanol:water partition coefficient of each etomidate analog was determined as previously described.[13]

Comparative Molecular Field Analysis

The low-energy conformer of etomidate and each etomidate analog was defined using MMFF94 force field utilizing an energy gradient convergence criterion of 0.01 kcal/mol with SybylX2.1.1 (Certara, USA). Partial electronic charges were calculated by the software using the Gasteiger–Hückel

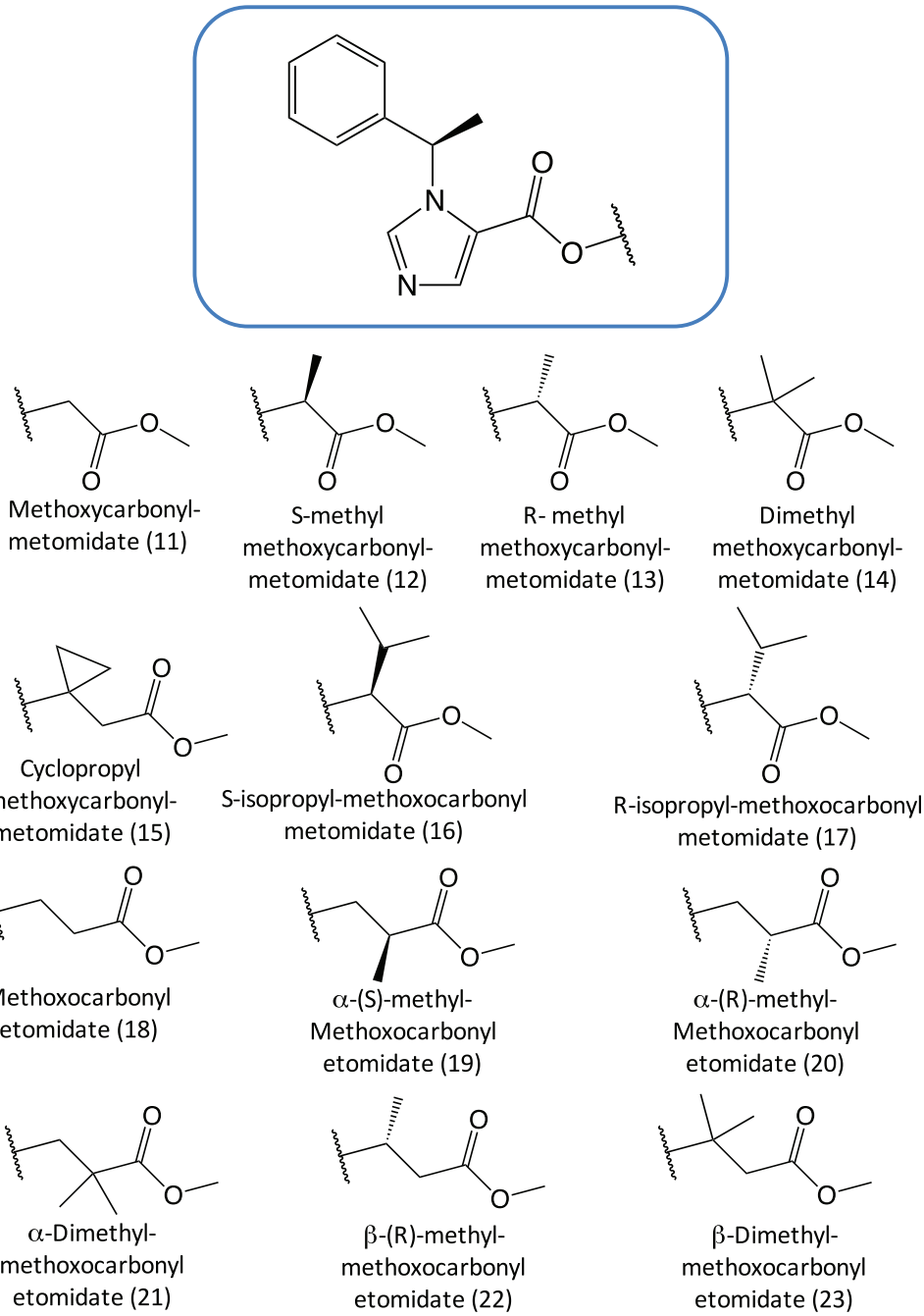

Fig. 2. Chemical structures of etomidate esters, their names, and their numerical designations. The etomidate pharmacophore is displayed in the *box* (*top*). The varying spacer that links the metabolically labile ester moiety to the etomidate pharmacophore is shown below the *box*.

method.[24] By using etomidate's structure as the template, each etomidate analog was then automatically aligned *in silico* to overlay its molecular shape, hydrogen-bonding capacities, and electrostatic properties with Surflex-Sim (Certara L.P.). When an imidazole ring was present in an etomidate analog, these alignments were further optimized by manually aligning this ring with that of etomidate.

Classic comparative molecular field analysis (CoMFA) interaction fields (steric and electrostatic fields) were calculated with SybylX2.1.1 using the default settings. The steric and electrostatic interaction energies were calculated on grid points of a regularly spaced three-dimensional lattice with a sp^3 carbon probe atom having a charge of +1 and a van der Waals radius of 1.52Å. The grid size had the software's default resolution of 2Å. Cutoffs were applied to both the steric and electrostatic interactions with energies at 30 kcal/mol. CoMFA region focusing was used to enhance the resolution of the model and improve its predictive power. In this

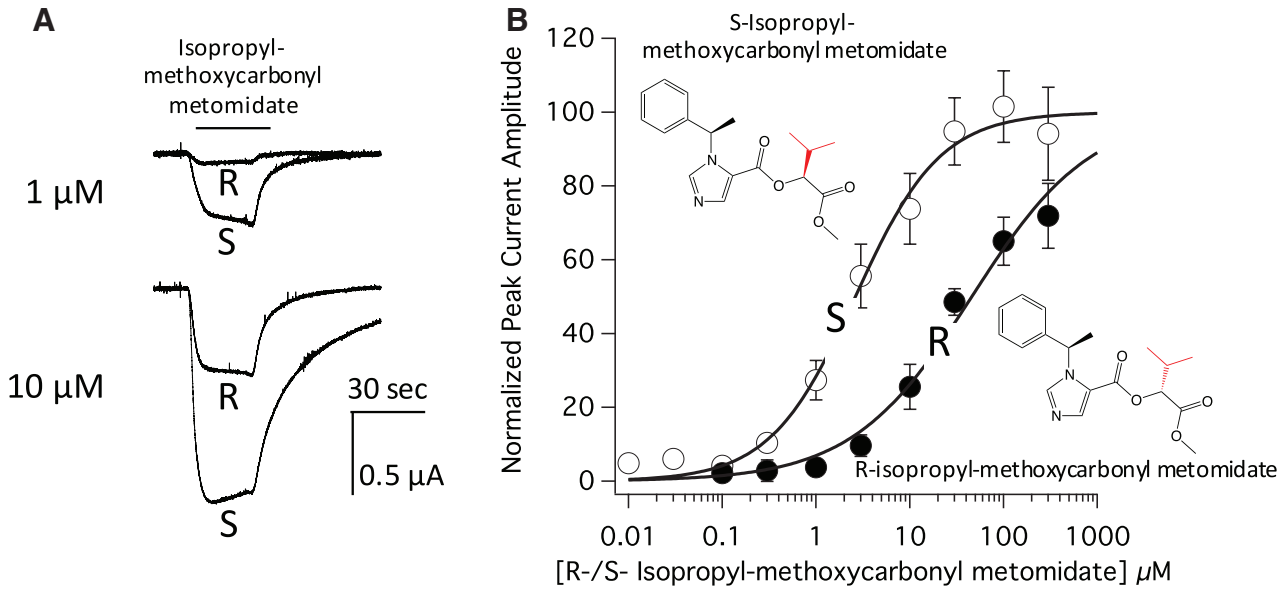

Fig. 3. Direct activation of $\alpha_1(L264T)\beta_3\gamma_2$ γ-aminobutyric acid type A ($GABA_A$) receptors expressed in oocytes by R-isopropyl-methoxycarbonyl metomidate and S-isopropyl-methoxycarbonyl metomidate. (*A*) Electrophysiologic traces recorded on perfusing an oocyte expressing $\alpha_1(L264T)\beta_3\gamma_2$ $GABA_A$ receptors with 1 (*top*) or 10 μM (*bottom*) S- or R-isopropyl-methoxycarbonyl metomidate. The same oocyte was used to obtain all four traces. (*B*) S- and R-isopropyl-methoxycarbonyl metomidate concentration–response relationships for $\alpha_1(L264T)\beta_3\gamma_2$ $GABA_A$ receptor direct activation. Each data point is the mean value (± SD) obtained from six different oocytes. In each *panel*, the chemical structures are shown as insets with the differences between analogs highlighted in *red*. The curves are fits of the two data sets to a Hill equation yielding half-maximal direct activating concentrations of 2.6 ± 3 and 46 ± 6 μM for S- and R-isopropyl-methoxycarbonyl metomidate, respectively ($P < 0.0001$).

procedure, the weightings of lattice points in the grid are modified by the software in an iterative fashion to enhance or reduce each point's contribution to subsequent analysis.

The partial least-squares approach was used to derive the three-dimensional quantitative structure–activity relationship, and cross-validation was performed using the leave-one-out method.[25] The optimum number of components (NC) that produced the lowest SE of predictions (SDEP) was determined, and the cross-validation correlation coefficient (q^2) was calculated. A coefficient of determination (r^2) was then defined from the relationship between the predicted and the experimental potencies using linear regression.

Pharmacophore Analysis

The five molecules with the lowest $GABA_A$ receptor EC_{50}s (*i.e.*, the five most potent $GABA_A$ receptor direct activators) were extracted from the alignment prepared for the $GABA_A$ receptor CoMFA analysis, and a pharmacophore model was constructed with unity (Certara L.P.). Such models describe the common features present in these ligands and the molecular interactions that they make with the protein that are important determinants of potency. For this analysis, we required that such interactions be present in at least four of the five high-potency molecules in the data set. We used a maximum volume constraint of 1 Å around each pharmacophore point. Thus, in some cases, a pharmacophore point on the ligand could not be associated with one at the receptor-binding site because the latter's volume exceeded the 1 Å cutoff (*i.e.*, there was too much uncertainty regarding the location of the receptor pharmacophore point). Aromatic and hydrophobic ligand domains were identified using rules in SybylX2.1.1 software. We then used MOLCAD (Cetara L.P.) to visualize the surface features and physical properties required for molecular recognition.

Statistical Analysis

All data are reported as mean ± SD. Sample sizes were chosen based on our previous experience.[13] Hypothesis testing was two tailed, and a P value less than 0.05 was considered to be statistically significant. Curve fitting to define $GABA_A$ receptor EC_{50}s and rat LORR ED_{50}s and their respective SDs were performed using Igor Pro 6.1 (Wavemetrics, USA). Linear regressions of logarithm-transformed data ($GABA_A$ receptor EC_{50}s and rat LORR ED_{50}s *vs.* hydrophobicity) were performed using Igor Pro 6.1. Statistical differences between the EC_{50}s of two compounds were assessed using an extra sum-of-squares F test with Prism 6 (Graphpad, USA). The sample sizes for data shown in all figures are indicated in the text. CoMFA statistics (NC, SDEP, q^2, and r^2) were calculated by SybylX2.1.1 software. There was no lost or missing data.

Results

Direct Activation of $GABA_A$ Receptors by Etomidate Analogs

All etomidate analogs directly activated $\alpha_1(L264T)\beta_3\gamma_2$ $GABA_A$ receptors expressed in oocytes in a concentration-dependent manner. Figure 3A shows representative electrophysiologic

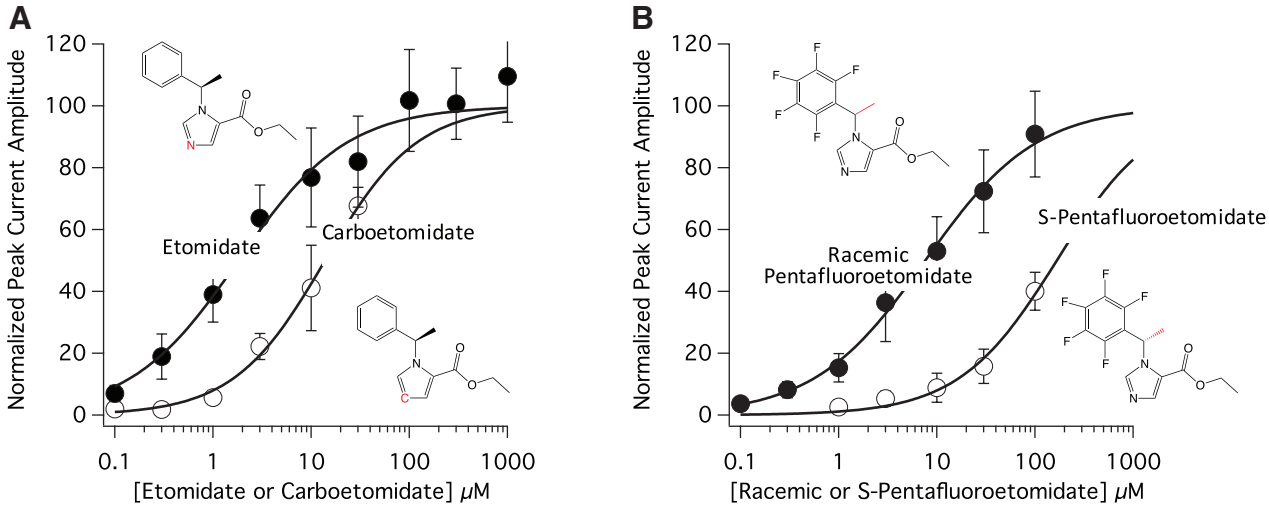

Fig. 4. (*A*) Etomidate and carboetomidate concentration–response relationships for α_1(L264T)$\beta_3\gamma_2$ γ-aminobutyric acid type A ($GABA_A$) receptor direct activation. Each data point is the mean value (± SD) obtained from four to six different oocytes. Data for etomidate was taken from Ref. 13. The curves are fits of the two data sets to a Hill equation yielding half-maximal direct activating concentrations of 1.83 ± 0.28 and 13.8 ± 0.9 μM for etomidate and carboetomidate, respectively ($P < 0.0001$). (*B*) Racemeic and S-pentafluoroetomidate concentration–response relationships for α_1(L264T)$\beta_3\gamma_2$ $GABA_A$ receptor direct activation. Each data point is the mean value (± SD) obtained from six different oocytes. The curves are fits of the two data sets to a Hill equation yielding half-maximal direct activating concentrations of 7.6 ± 0.6 and 166 ± 25 μM, respectively ($P < 0.0001$). In each *panel*, the chemical structures are shown as *insets* with the differences between analogs highlighted in *red*.

traces recorded on perfusing a single oocyte with the diastereomeric etomidate ester pair R-isopropyl-methoxycarbonyl metomidate and S-isopropyl-methoxycarbonyl metomidate at concentrations of 1 (top) and 10 μM (bottom). At 1 μM, the R- and S-diastereomers evoked currents having peak amplitudes of 0.041 and 0.29 μA, respectively. At 10 μM, they evoked respective currents having peak amplitudes of 0.36 and 0.90 μA, respectively. For the two diastereomers, figure 3B plots the concentration–response relationship for peak current activation (mean ± SD, n = 6 oocytes per data point). For both diastereomers, the normalized peak current response increased with concentration. At a near saturating aqueous concentration (100 μM), S- (but not R-) isopropyl-methoxycarbonyl metomidate evoked currents that approximated those evoked by a maximally activating concentration (100 μM) of GABA. A fit of these concentration–response curves to equation 1 yielded EC_{50}s for direct activation of 2.6 ± 0.3 and 46 ± 6 μM for S- and R-isopropyl-methoxycarbonyl metomidate, respectively ($P < 0.0001$).

Figure 4A plots the concentration–response relationships for peak current activation by etomidate and carboetomidate, a pyrrole etomidate analog that does not suppress adrenocortical function. The normalized peak current amplitude increased with both etomidate and carboetomidate concentrations. However, similar to R-isopropyl-methoxycarbonyl metomidate, carboetomidate's relatively low potency and aqueous solubility limited our studies to carboetomidate concentrations that activated (at most) only 68 ± 6% of $GABA_A$ receptors. From these concentration–response curves, we determined that carboetomidate's potency for directly activating $GABA_A$ receptors is approximately one eighth that of etomidate with EC_{50}s of 13.8 ± 0.9 μM for carboetomidate and 1.83 ± 0.28 μM for etomidate ($P < 0.0001$).

Figure 4B plots the concentration–response relationships for peak current activation by the fluorinated etomidate analog S-pentafluoroetomidate. This figure also plots this relationship for racemic pentafluoroetomidate, which contains equal quantities of the R- and S-enantiomers. The EC_{50} for the S-enantiomer was 22-fold higher than that of the racemic mixture (166 ± 25 *vs.* 7.6 ± 0.6 μM, respectively; $P < 0.0001$). This implies that essentially all of the directly activated current recorded during application of the racemic mixture was attributable to the R- enantiomer and that R-enantiomer's EC_{50} is approximately 3.8 μM (*i.e.*, one half the EC_{50} of the racemic mixture).

Table 1 gives the $GABA_A$ receptor EC_{50}s for etomidate and all of the etomidate analogs that we have characterized to date, along with their physical properties (*i.e.*, molecular weights, molecular volumes, and octanol:buffer partition coefficients) and their hypnotic ED_{50}s measured in Sprague Dawley rats. We have reported some of these values previously and provided the references for these published values in the table.

Although hydrophobicity has long been considered to be an important determinant of *in vitro* and *in vivo* anesthetic potency, figure 5 shows that the correlation between the $GABA_A$ receptor potencies of etomidate and etomidate analogs and their octanol:buffer partition coefficients is rather poor.[26–28] A linear fit of the logarithm-transformed values of this relationship yielded a slope that is not significantly different from 0 (0.13 ± 0.20, $P = 0.5271$) and an r^2 of only 0.019. An analogous linear fit of the logarithm-transformed relationship between hypnotic potency in rats

Table 1. Molecular and Pharmacologic Properties of Etomidate and Etomidate Analogs

Compound*	Compound Name	Molecular Weight (g/mol)	Molecular Volume (Å)†	Octanol:Buffer Partition Coefficient	$GABA_A$ Receptor EC_{50}* (μM)	Hypnotic ED_{50} (mg/kg)
1	Etomidate	244.29	239.89	731 ± 72 (13)	1.83 ± 0.28 (13)	0.47 ± 0.17 (13)
2	Metomidate	230.26	229.88	380 ± 48	4.4 ± 0.7	0.73 ± 0.50
3	S-etomidate	244.29	247.38	711 ± 90 (13)	57.0 ± 5.1 (13)	5.2 ± 0.9 (13)
4	Dihydrogen etomidate	230.26	224.38	388 ± 32 (13)	161 ± 13 (13)	5.2 ± 1 (13)
5	Cyclopropyl etomidate	256.3	254.28	458 ± 45 (13)	67.6 ± 8.1 (13)	5.2 ± 0.7 (13)
6	Carboetomidate	243.3	251.06	15,000 ± 3,700 (20)	13.8 ± 0.9	7.7 ± 0.8 (18)
7	4-Pyridine carboetomidate	244.29	755.12	753 ± 63	335 ± 36	25.0 ± 0.3
8	Racemic pentafluoroetomidate	334.24	N/A	860 ± 260	7.6 ± 0.6	1.7 ± 0.4
9	S-pentafluoroetomidate	334.24	268.04	880 ± 220	167 ± 25	11.1 ± 0.8
10	R-pentafluoroetomidate	334.24	276.62	870‡	3.8‡	0.9‡
11	Methoxycarbonyl metomidate	288.3	284.33	159 ± 15 (19)	38 ± 2	11.1 ± 0.8 (19)
12	S-methyl-methoxycarbonyl metomidate	302.33	294.77	330 ± 16 (19)	9.4 ± 0.8	3.5 ± 0.4 (19)
13	R-methyl- methoxycarbonyl metomidate	302.33	293.08	380 ± 15 (19)	8.2 ± 0.9	9.6 ± 1.9 (19)
14	Dimethyl-methoxycarbonyl metomidate	316.35	303.45	660 ± 110 (19)	1.6 ± 0.4	0.72 ± 0.16 (19)
15	Cyclopropyl methoxycarbonyl metomidate	314.34	302.96	420 ± 11 (19)	3.8 ± 0.4 (5)	0.69 ± 0.04 (19)
16	(S)-isopropyl-methoxycarbonyl metomidate	330.38	328.88	2,860 ± 67 (19)	2.6 ± 0.3	1.2 ± 0.2 (19)
17	(R)-isopropyl-methoxycarbonyl metomidate	330.38	337.5	3,830 ± 310 (19)	46 ± 6	3.6 ± 0.8 (19)
18	Methoxycarbonyl etomidate	302.33	309.63	190 ± 25 (19)	20 ± 2	5.3 ± 1.5 (19)
19	α-(S)-methyl methoxycarbonyl etomidate	316.35	317.55	530 ± 170 (19)	11 ± 2	3.1 ± 0.4 (19)
20	α-(R)-methyl-methoxycarbonyl etomidate	316.35	310.3	670 ± 120 (19)	35 ± 12	5.2 ± 0.5 (19)
21	α-Dimethyl-methoxycarbonyl etomidate	330.38	328.51	2,240 ± 150 (19)	5.5 ± 0.6	2.4 ± 1 (19)
22	β-(R)-methyl- methoxycarbonyl etomidate	316.35	319.02	500 ± 24 (19)	11 ± 1	3.5 ± 0.6 (19)
23	β-Dimethyl-methoxycarbonyl etomidate	330.38	326.65	1,580 ± 40 (19)	1.7 ± 0.2	1.9 ± 0.3 (19)

Numbers in parentheses are the references for previously published values.

*Hill coefficients averaged 0.83 ± 0.22 (range, 0.539–1.54). †van der Waals volume calculated by SybylX2.1.1. ‡Value estimated from studies using the racemic mixture and the S-enantiomer.

EC_{50} = concentration that evokes a peak current amplitude that is 50% of that produced by 100 μM GABA; ED_{50} = dose that produces loss of righting reflexes in 50% of rats; $GABA_A$ = γ-aminobutyric acid type A.

and octanol:buffer partition coefficient similarly yielded a slope that was not significantly different from 0 (0.09 ± 0.30, $P = 0.7562$) and an r^2 of only 0.005 (data not shown).

Three-dimensional Quantitative Structure-activity Analysis of Etomidate Analog Potency

We used CoMFA to identify the structural elements in our etomidate analogs (fig. 6) that account for their widely ranging (91-fold) $GABA_A$ receptor potencies. Figure 7 shows the final alignment of etomidate and the 21 different etomidate analogs along with the resulting CoMFA contour maps. Figure 7A shows the steric contour map depicting where bulky substituents increase (green) or decrease (yellow) $GABA_A$ receptor potency. Figure 7B shows the electrostatic contour map depicting where electronegative substituents (red) or electropositive substituents (blue) increase $GABA_A$ receptor potency. The model had good predictive ability as assessed by leave-one-out cross-validation with values of $q^2 = 0.458$, NC = 4, and SDEP = 0.458. Figure 8 shows the correlation between the $GABA_A$ receptor EC_{50} values predicted by the CoMFA model and the experimentally derived $GABA_A$ receptor EC_{50} values. The model explained 91.2% of the variance in the observed activities of the etomidate analogs with values of $r^2 = 0.912$, NC = 4, and SDEP = 0.227.

The identical alignment was used to identify the structural features of our etomidate analogs that account for their widely ranging (53-fold) hypnotic potencies in rats. Figure 9A shows the steric contour map depicting where bulky substituents increase (green) or decrease (yellow) hypnotic potency. Figure 9B shows the electrostatic contour map depicting where electronegative substituents (red) or electropositive substituents (blue)

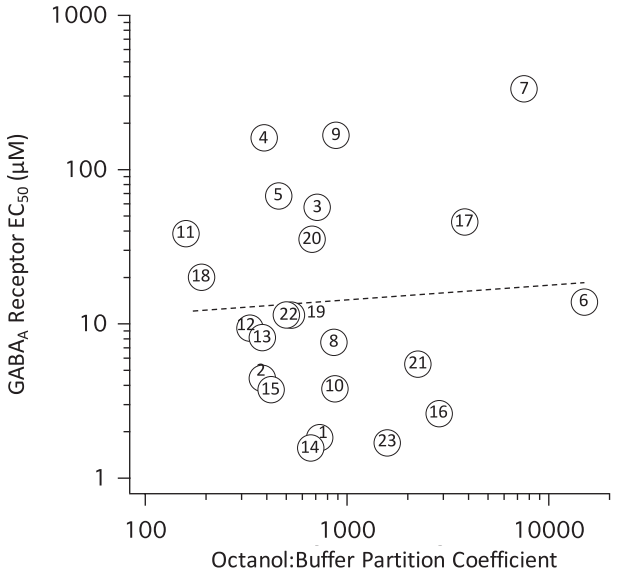

Fig. 5. Relationship between the half-maximal direct activating concentration of etomidate and etomidate analogs (EC_{50}) and their octanol:water partition coefficients. The *dashed line* is a linear fit of the logarithm-transformed data. The slope of the fitted line was 0.13 ± 0.20 μM, and the coefficient of determination (r^2) was 0.019. The name and structure of each numbered compound is given in table 1.

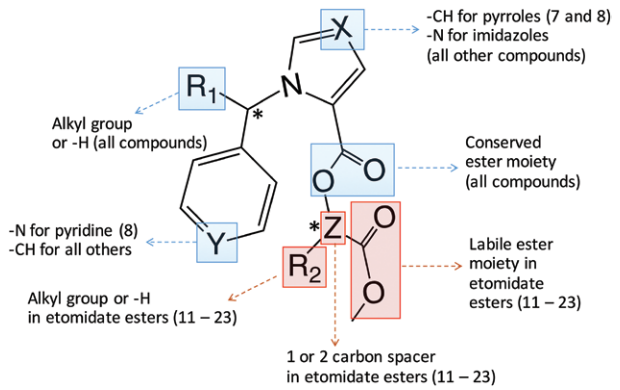

Fig. 6. Generic structure for all etomidate analogs. The *blue boxes* highlight the location where the molecular structure of the analogs varied. *Red boxes* highlight structural elements found only in the etomidate ester series of compounds. The *asterisks* show carbons that were chiral centers in some of our compounds.

increase hypnotic potency. Figure 10 shows the correlation between the hypnotic ED_{50} values predicted by the CoMFA model and the experimentally derived hypnotic ED_{50} values. The CoMFA model explained 97.3% of the variance in the observed hypnotic potencies (r^2 = 0.973, NC = 5, and SDEP = 0.093) and showed good predictive capability with leave-one-out validation (q^2 = 0.521, NC = 5, and SDEP = 0.377).

Visual comparison of the contour maps for *in vitro* $GABA_A$ receptor potency (fig. 7) and *in vivo* hypnotic potency (fig. 9) reveals certain similarities. For example, in both steric contour maps (figs. 7A and 9A), there is a yellow contour near the chiral carbon located between the phenyl and the imidazole rings indicating that the S-form is sterically disfavored. There is a similar yellow contour near the spacer located between the two ester moieties of etomidate esters indicating that the R-form is sterically disfavored. The "steric penalty" for being in the disfavored enantiomeric form at either of these chiral centers was a reduction in receptor and hypnotic potencies of as much as 1 to 2 orders of magnitude (table 1). For both steric contour maps, there is also a green contour around the alkyl groups of the etomidate ester spacer (represented as R_2 in fig. 6) indicating that bulky substituents in this region increase both receptor and hypnotic potencies. In both electrostatic contour maps (figs. 7B and 9B), there is a red contour around the conserved carboxylate ester showing favored negative charge related to the carbonyl oxygen and a blue contour around the distal ester of etomidate esters showing favored positive charge relating to the carbonyl carbon.

Three-dimensional Pharmacophore Analysis of Etomidate Analog

To better understand the drug–receptor interactions that mediate high $GABA_A$ receptor potency, we built a pharmacophore model using the five most potent $GABA_A$ receptor direct activators shown on table 1. Because four of five of these compounds have an additional carboxylate ester moiety (they are etomidate esters), we allowed a 20% miss rate (one of five molecules) to allow optional pharmacophore features to be included in the final model. This model, along with the five most potent compounds, is shown in figure 11. The model identified four common features and one optional feature in these compounds. The first feature is the basic nitrogen in the imidazole ring, which was identified as a hydrogen bond acceptor for a donor in the receptor. This interaction explains why etomidate's potency is 1 to 2 orders of magnitude higher than those of the pyrrole analogs of carboetomidate and 4-pyridine carboetomidate. The second feature is the phenyl ring, which is hydrophobic and explains the 24-fold higher potency of carboetomidate compared with 4-pyridine carboetomidate. The third and fourth features are the two conserved oxygens that form the ester adjacent to the imidazole ring. Similar to the imidazole nitrogen, the carbonyl oxygen of this ester was identified as a hydrogen bond acceptor for a donor in the receptor. The distance between these two donors in the receptor was determined to be 9.36 Å by the model. The final feature is the distal ester found in the etomidate esters, which was identified as optional hydrogen bond acceptor. The van der Waals surface of these five most potent compounds was then calculated, and their lipophilic potentials were mapped onto that surface. Figure 12 shows that surface, along with the structures of those five most potent compounds, the pharmacophore model, and the CoMFA contours for $GABA_A$ receptor potency. As the yellow contours denote regions where bulky

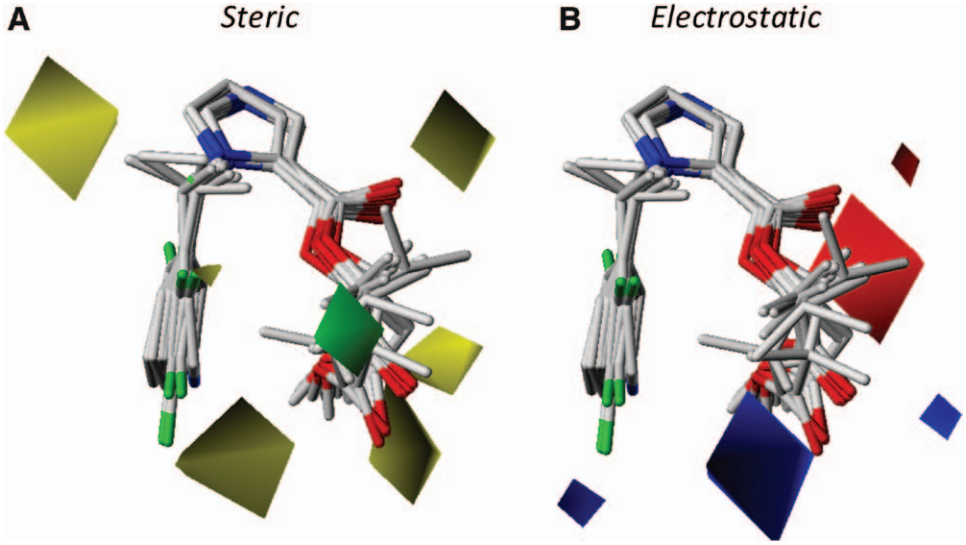

Fig. 7. Alignment of etomidate and etomidate analogs and comparative molecular field analysis contour maps for direct activation of α_1(L264T)$\beta_3\gamma_2$ γ-aminobutyric acid type A ($GABA_A$) receptors. (*A*) Steric field contour map. The *green contours* represent regions where bulky substituents increase analog potency, whereas *yellow contours* represent regions where they decrease potency. (*B*) Electrostatic contour map. The *blue contours* represent regions where electropositive substituents increase analog potency, whereas *red contours* represent regions where electronegative substituents increase potency.

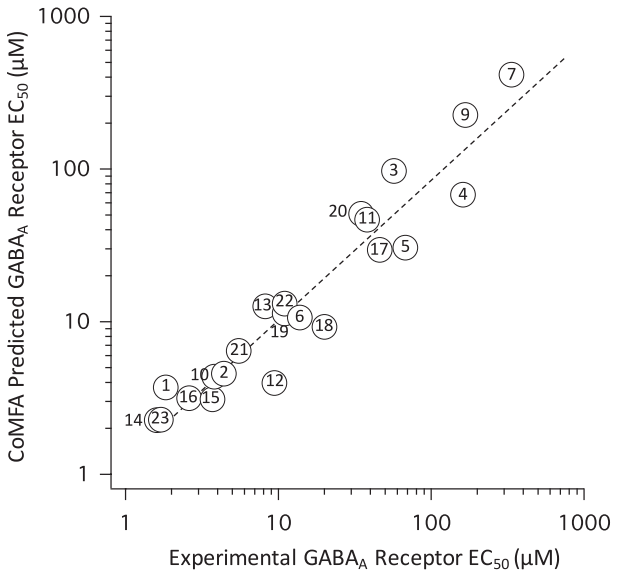

Fig. 8. Relationship between the half-maximal direct activating concentration (EC_{50}) predicted by our comparative molecular field analysis (CoMFA) model and that determined experimentally from our electrophysiologic studies. The experimental EC_{50} for each analog was defined using α_1(L264T)$\beta_3\gamma_2$ γ-aminobutyric acid type A ($GABA_A$) receptors expressed in oocytes. The *dashed line* is a linear fit of the logarithm-transformed data. The slope of the fitted line was 0.912 ± 0.063, and the coefficient of determination (r^2) was 0.91. The name and structure of each numbered compound is given in table 1.

substituents reduce potency (presumably because steric hindrance reduces binding affinity), they are considered to represent (part of) the lining of the etomidate-binding pocket. Conversely, the green contour denotes the only region in our receptor model where bulky substituents increase potency. As this bulk is in the form of hydrophobic alkyl groups in all of our compounds (R_2 in fig. 6), we conclude that this part of the binding pocket is relatively hydrophobic and spacious as it can even accommodate an isopropyl group, which was the largest alkyl group that we studied.

Discussion

Etomidate is widely believed to produce its hypnotic effects by binding to the $GABA_A$ receptor and enhancing its function. This conclusion is most strongly supported by studies showing that (1) etomidate's R- and S-enantiomers produce hypnosis with potencies that correlate with their $GABA_A$ receptor affinities and potencies; and (2) an amino acid mutation that abolishes etomidate's ability to enhance $GABA_A$ receptor function (N265M on the β subunit) significantly reduces the etomidate sensitivities of transgenic mice containing that mutation.[3,8,13,16,29] This amino acid, along with others, may contribute to an etomidate-binding site on the $GABA_A$ receptor's open state that is located in the membrane-spanning receptor domains between the α and β subunits.[5–7]

There have been few studies to define the anesthetic structural features required for high-affinity binding to the $GABA_A$ receptor's etomidate-binding site and/or modulation of the receptor's function. Competition studies using an etomidate photoaffinity label indicate that propofol and barbiturates bind to that site with lower affinity than R-etomidate, and the steroid anesthetic alphaxalone does not bind to that site at all.[8] Thus, this binding site can distinguish among classes of general anesthetics. The *in vitro* electrophysiologic data presented in this study demonstrate that even within a single anesthetic class (*i.e.*, etomidate), this site exhibits

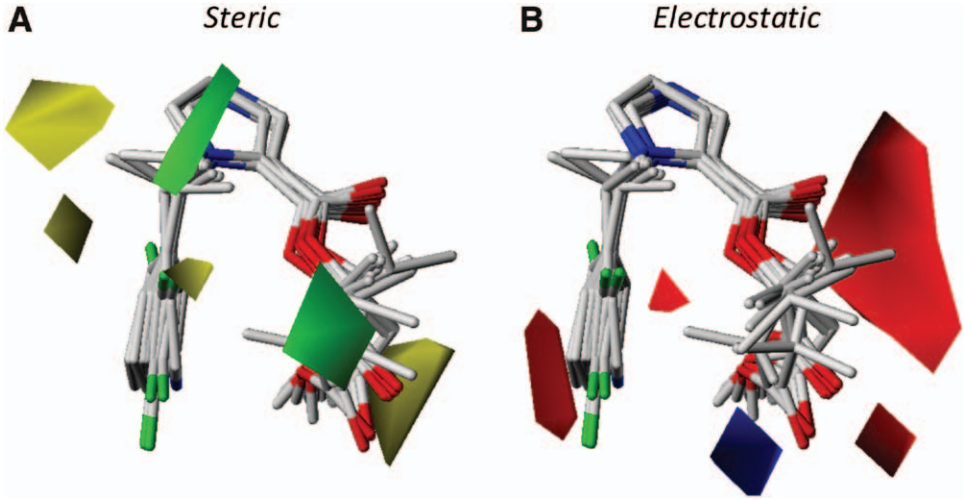

Fig. 9. Alignment of etomidate and etomidate analogs and comparative molecular field analysis contour maps for loss of righting reflexes in rats. (*A*) Steric field contour map. The *green contours* represent regions where bulky substituents increase analog potency, whereas *yellow contours* represent regions where they decrease potency. (*B*) Electrostatic contour map. The *blue contours* represent regions where electropositive substituents increase analog potency, whereas *red contours* represent regions where electronegative substituents increase potency.

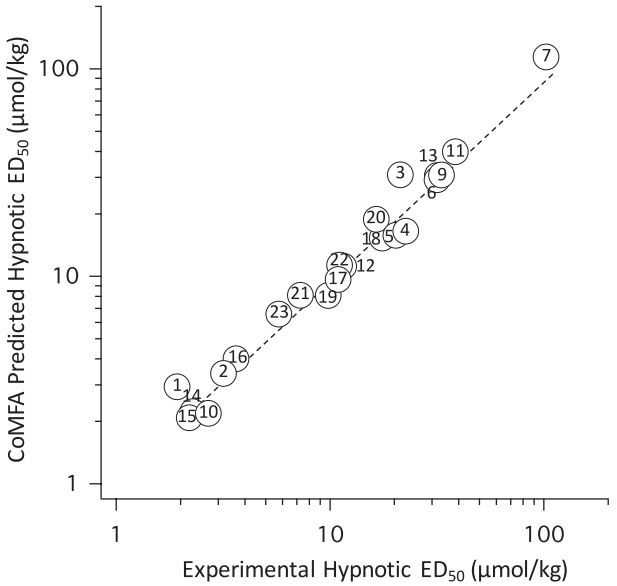

Fig. 10. Relationship between the median effective dose that produces loss of righting reflexes in rats (ED_{50}) predicted by our comparative molecular field analysis (CoMFA) model and that determined experimentally in rats. The *dashed line* is a linear fit of the logarithm-transformed data. The slope of the fitted line was 0.972 ± 0.036, and the coefficient of determination (r^2) was 0.97. The name and structure of each numbered compound is given in table 1.

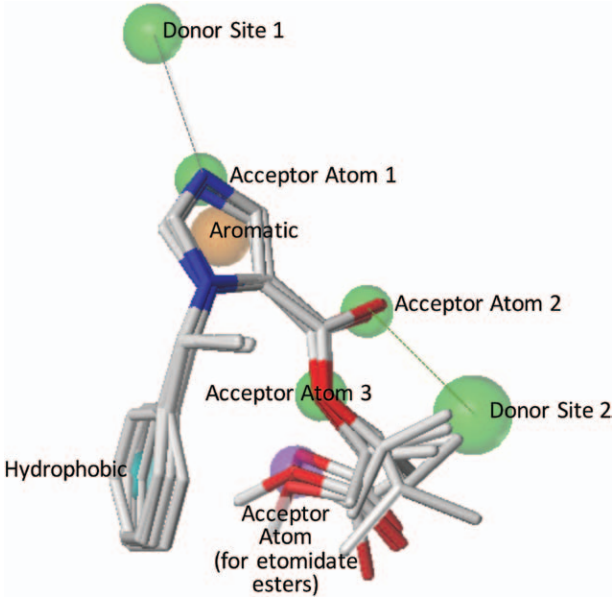

Fig. 11. Pharmacophore model of etomidate analogs overlaying the five compounds having the highest γ-aminobutyric acid type A ($GABA_A$) receptor potencies. The hydrophobic regions are *blue*, the aromatic regions are *orange*, the acceptor atom–donor site interactions are *green*. For the etomidate esters, there is also an acceptor atom–donor site interaction that is shown in *purple*. The *dotted lines* show interactions where a pharmacophore point on the ligand could be associated with one on the receptor-binding site because the volume constraint of the latter also fell within the 1-Å limit. The distance between donor site 1 and donor site 2 is 9.36 Å.

considerable selectivity as evidenced by the widely (91-fold) ranging $GABA_A$ receptor potencies of our etomidate analogs that could not be simply explained by their different hydrophobicities. The widely ranging $GABA_A$ receptor potencies of our analogs were matched by a similarly large (53-fold) range in their hypnotic potencies, and a logarithmic plot of $GABA_A$ receptor potency *versus* hypnotic potency (fig. 13) showed a significant correlation (r^2 = 0.72) between these two potency measurements. The slope of this relationship was significantly different from 0 (P < 0.0001) and near unity (1.22 ± 0.18), indicating that (in general) when an

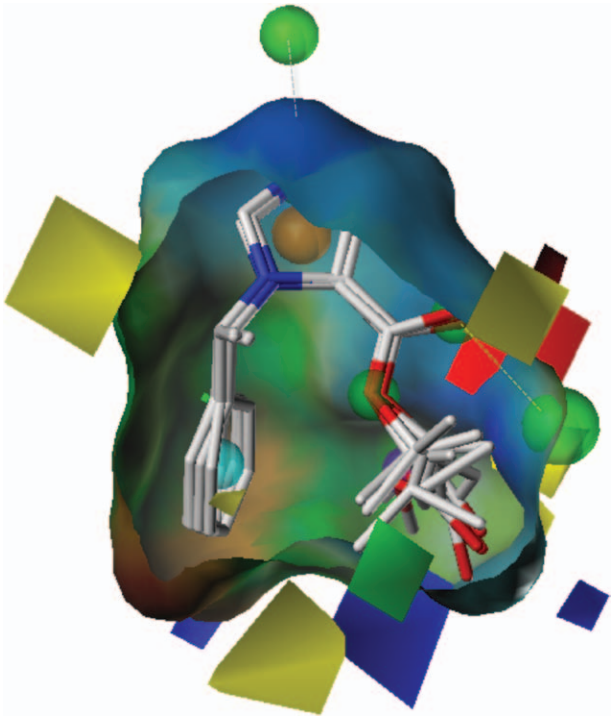

Fig. 12. Pharmacophore model of etomidate analogs with the merged surface of the five compounds having the highest γ-aminobutyric acid type A ($GABA_A$) receptor potencies. The surface colors are based on lipophilic potential ranging from *brown* (highly lipophilic) to *blue* (highly hydrophilic), and z-clipping was applied to the surface to match the $GABA_A$ receptor comparative molecular field analysis contour maps. The *dotted lines* show interactions where a pharmacophore point on the ligand could be associated with one on the receptor-binding site because the volume constraint of the latter also fell within the 1-Å limit.

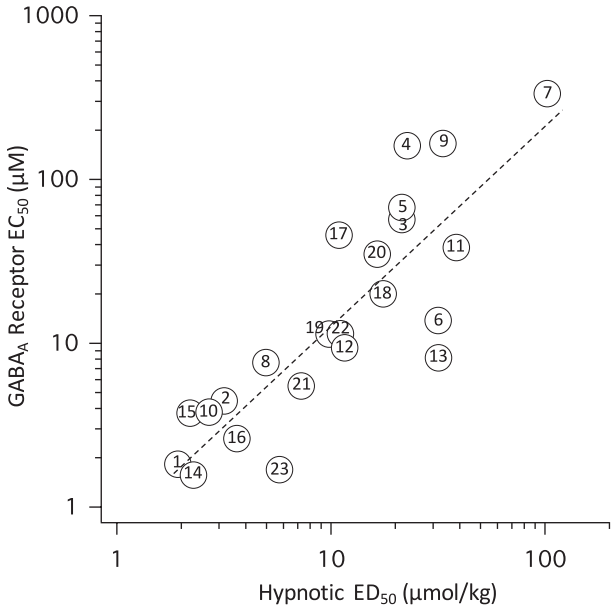

Fig. 13. Relationship between *in vitro* γ-aminobutyric acid type A ($GABA_A$) receptor and *in vivo* hypnotic potencies of etomidate and etomidate analogs. Each compound's $GABA_A$ receptor potency is defined as the half-maximal direct activating concentration (EC_{50}), and its hypnotic potency is defined as the median effective dose that produces loss of righting reflexes in rats (ED_{50}). The *dashed line* is a linear fit of the logarithm-transformed data. The slope of the fitted line was 1.22 ± 0.18, and the coefficient of determination (r^2) was 0.72.

etomidate analog's $GABA_A$ receptor potency doubled, its hypnotic potency also doubled. These findings are consistent with a direct cause-and-effect relationship between $GABA_A$ receptor enhancement by etomidate analogs and the production of *in vivo* hypnosis.

Our computational studies provide additional details regarding the specific anesthetic structural features present in high-potency modulators of the $GABA_A$ receptor function and define the important interactions that etomidate analogs make with amino acids that form the etomidate-binding site on the receptor. For example, our studies show that the basic nitrogen in the imidazole ring and the carboxylate ester adjacent to that ring are important hydrogen bond acceptors for donors in the receptor. Although we do not know the identity of these amino acids, it is tempting to speculate that one of these donor amino acids is β_3N265. This could explain the results of allosteric modeling studies indicating that mutating this asparagine to a methionine (which is not a hydrogen bond donor) reduces etomidate's affinity for open-state $GABA_A$ receptors by orders of magnitude, whereas mutating it to a serine (which can be hydrogen bond donor) reduces etomidate's affinity by only half.[30–32] It was concluded from those studies that the reduced etomidate sensitivity of the serine-containing mutant (β_3N265S) measured in electrophysiologic studies is primarily because of a reduction in etomidate's efficacy rather than its binding affinity. Our computational studies also indicated that (1) the phenyl ring engages in a hydrophobic interaction with hydrophobic amino acid residues in the binding site; (2) there is chiral selectivity around the carbon located between the phenyl and imidazole rings; and (3) in the case of etomidate esters, there is a hydrogen bond interaction between the distal carboxylate ester and a donor on the protein, and chiral selectivity around the spacer that links the distal ester to the etomidate pharmacophore.

The computational modeling approach utilized in the present studies (CoMFA) to define ligand–protein interactions are distinct from—but complimentary to—computational docking studies.[33–36] In the CoMFA approach, there are no *a priori* assumptions regarding the nature of the protein-binding site. Instead, the molecular (*i.e.*, steric and electrostatic) interactions between a set of ligands and their protein-binding site are identified from the relationship between ligand molecular structure and binding affinity, and the latter often quantified experimentally using a functional assay.[37–39] This technique allows one to construct a pharmacophore model that explains the observed biologic activity and provides information about the molecular forces

involved in binding. There are several important limitations of this approach. These limitations include potential uncertainty regarding the alignment of ligands, particularly when the structures of ligands in a data set vary widely. In addition, the conformation of a ligand may change on protein binding. Consequently, the low-energy states calculated by CoMFA may differ from the actual protein-bound states. Such inherent limitations may explain why the correlations that we observed between model-predicted and experimental potency values were good, but not perfect. In contrast, docking studies attempt to fit a ligand into a defined protein-binding site *in silico*. They are typically agnostic to ligand potency and can utilize a single ligand but require a high-resolution structural model of the binding site to calculate the interaction energy between ligand and protein. Unfortunately, the structures of open-state heteromeric $GABA_A$ receptors have not yet been defined at high resolution. However, progress in that direction is being made through the construction of homology models that seek to approximate the receptor's structure by utilizing structurally similar proteins.[33,34] With further refinement and validation of these models or the production of a high-resolution heteromeric $GABA_A$ receptor crystal structure, it may be possible to unambiguously identify amino acids at the etomidate-binding site that are the important determinants of receptor (and therefore hypnotic) potency and account for our pharmacophore model.

In summary, we have measured the $GABA_A$ receptor potencies of a series of etomidate analogs and found that their potencies range by 91-fold. The receptor potencies of these analogs correlated with their hypnotic potencies but not with their hydrophobicities. CoMFA indicated that there are multiple structural elements in these etomidate analogs that define their $GABA_A$ receptor potencies. These include the imidazole nitrogen and carboxylate ester (which act as hydrogen bond acceptors), the phenyl ring (which can engage in hydrophobic interactions), the chiral carbon located between the phenyl and the imidazole rings (the R configuration has higher potency), and the chiral carbon located between the etomidate pharmacophore and the distal ester in etomidate esters (the S configuration has higher potency). Modifying any of one of these structural elements can alter receptor potency by an order of magnitude or more.

Acknowledgments

This study was funded by grant R01-GM087316 from the National Institutes of Health, Bethesda, Maryland, and the Department of Anesthesia, Critical Care, and Pain Medicine, Massachusetts General Hospital, Boston, Massachusetts.

Competing Interests

The Massachusetts General Hospital, Boston, Massachusetts, has published and submitted patent applications for certain etomidate analogs. Drs. Raines and Husain are inventors of this technology. They and their laboratories have received income related its development. This conflict is being managed by the Partners Healthcare Office for Interactions with Industry. The other authors declare no competing interests.

Correspondence

Address correspondence to Dr. Raines: Department of Anesthesia, Critical Care, and Pain Medicine, Massachusetts General Hospital, 55 Fruit Street, GRB444, Boston, Massachusetts 02114. draines@partners.org. Information on purchasing reprints may be found at www.anesthesiology.org or on the masthead page at the beginning of this issue. Anesthesiology's articles are made freely accessible to all readers, for personal use only, 6 months from the cover date of the issue.

References

1. Reynolds DS, Rosahl TW, Cirone J, O'Meara GF, Haythornthwaite A, Newman RJ, Myers J, Sur C, Howell O, Rutter AR, Atack J, Macaulay AJ, Hadingham KL, Hutson PH, Belelli D, Lambert JJ, Dawson GR, McKernan R, Whiting PJ, Wafford KA: Sedation and anesthesia mediated by distinct GABA(A) receptor isoforms. J Neurosci 2003; 23:8608–17
2. Belelli D, Lambert JJ, Peters JA, Wafford K, Whiting PJ: The interaction of the general anesthetic etomidate with the gamma-aminobutyric acid type A receptor is influenced by a single amino acid. Proc Natl Acad Sci USA 1997; 94:11031–6
3. Tomlin SL, Jenkins A, Lieb WR, Franks NP: Stereoselective effects of etomidate optical isomers on gamma-aminobutyric acid type A receptors and animals. Anesthesiology 1998; 88:708–17
4. Forman SA: Clinical and molecular pharmacology of etomidate. Anesthesiology 2011; 114:695–707
5. Ge R, Pejo E, Gallin H, Jeffrey S, Cotten JF, Raines DE: The pharmacology of cyclopropyl-methoxycarbonyl metomidate: A comparison with propofol. Anesth Analg 2014; 118:563–7
6. Li GD, Chiara DC, Sawyer GW, Husain SS, Olsen RW, Cohen JB: Identification of a GABAA receptor anesthetic binding site at subunit interfaces by photolabeling with an etomidate analog. J Neurosci 2006; 26:11599–605
7. Chiara DC, Dostalova Z, Jayakar SS, Zhou X, Miller KW, Cohen JB: Mapping general anesthetic binding site(s) in human α1β3 γ-aminobutyric acid type A receptors with [^{3}H]TDBzl-etomidate, a photoreactive etomidate analogue. Biochemistry 2012; 51:836–47
8. Chiara DC, Jayakar SS, Zhou X, Zhang X, Savechenkov PY, Bruzik KS, Miller KW, Cohen JB: Specificity of intersubunit general anesthetic-binding sites in the transmembrane domain of the human α1β3γ2 γ-aminobutyric acid type A (GABAA) receptor. J Biol Chem 2013; 288:19343–57
9. Hill-Venning C, Belelli D, Peters JA, Lambert JJ: Subunit-dependent interaction of the general anaesthetic etomidate with the gamma-aminobutyric acid type A receptor. Br J Pharmacol 1997; 120:749–56
10. Rüsch D, Zhong H, Forman SA: Gating allosterism at a single class of etomidate sites on alpha1beta2gamma2L GABA A receptors accounts for both direct activation and agonist modulation. J Biol Chem 2004; 279:20982–92
11. Forman SA: Monod-Wyman-Changeux allosteric mechanisms of action and the pharmacology of etomidate. Curr Opin Anaesthesiol 2012; 25:411–8
12. Guitchounts G, Stewart DS, Forman SA: Two etomidate sites in α1β2γ2 γ-aminobutyric acid type A receptors contribute equally and noncooperatively to modulation of channel gating. Anesthesiology 2012; 116:1235–44
13. Pejo E, Santer P, Jeffrey S, Gallin H, Husain SS, Raines DE: Analogues of etomidate: Modifications around etomidate's chiral carbon and the impact on *in vitro* and *in vivo* pharmacology. Anesthesiology 2014; 121:290–301

14. Tomlin SL, Jenkins A, Lieb WR, Franks NP: Preparation of barbiturate optical isomers and their effects on GABA(A) receptors. Anesthesiology 1999; 90:1714–22
15. Davies PA, Kirkness EF, Hales TG: Modulation by general anaesthetics of rat GABAA receptors comprised of alpha 1 beta 3 and beta 3 subunits expressed in human embryonic kidney 293 cells. Br J Pharmacol 1997; 120:899–909
16. Belelli D, Muntoni AL, Merrywest SD, Gentet LJ, Casula A, Callachan H, Madau P, Gemmell DK, Hamilton NM, Lambert JJ, Sillar KT, Peters JA: The *in vitro* and *in vivo* enantioselectivity of etomidate implicates the GABAA receptor in general anaesthesia. Neuropharmacology 2003; 45:57–71
17. Cotten JF, Husain SS, Forman SA, Miller KW, Kelly EW, Nguyen HH, Raines DE: Methoxycarbonyl-etomidate: A novel rapidly metabolized and ultra-short-acting etomidate analogue that does not produce prolonged adrenocortical suppression. Anesthesiology 2009; 111:240–9
18. Cotten JF, Forman SA, Laha JK, Cuny GD, Husain SS, Miller KW, Nguyen HH, Kelly EW, Stewart D, Liu A, Raines DE: Carboetomidate: A pyrrole analog of etomidate designed not to suppress adrenocortical function. Anesthesiology 2010; 112:637–44
19. Husain SS, Pejo E, Ge R, Raines DE: Modifying methoxycarbonyl etomidate inter-ester spacer optimizes *in vitro* metabolic stability and *in vivo* hypnotic potency and duration of action. Anesthesiology 2012; 117:1027–36
20. Pejo E, Cotten JF, Kelly EW, Le Ge R, Cuny GD, Laha JK, Liu J, Lin XJ, Raines DE: *In vivo* and *in vitro* pharmacological studies of methoxycarbonyl-carboetomidate. Anesth Analg 2012; 115:297–304
21. Ge RL, Pejo E, Haburcak M, Husain SS, Forman SA, Raines DE: Pharmacological studies of methoxycarbonyl etomidate's carboxylic acid metabolite. Anesth Analg 2012; 115:305–8
22. Godefroi EF, Janssen PA, Vandereycken CA, Vanheertum AH, Niemegeers CJ: DL-1-(1-arylalkyl)imidazole-5-carboxylate esters. A novel type of hypnotic agents. J Med Chem 1965; 8:220–3
23. Waud DR: On biological assays involving quantal responses. J Pharmacol Exp Ther 1972; 183:577–607
24. Gasteiger J, Marsili M: Iterative partial equalization of orbital electronegativity—A rapid access to atomic charges. Tetrahedron 1980; 36:3219–28
25. Stone M: Cross-validatory choice and assessment of statistical predictions. J R Stat Soc Series B Stat Methodol 1974; 36:111–47
26. Meyer H: Theorie der alkohonarkose. Arch Exp Pathol Pharmacol 1899; 42:109–18
27. Barker JL: Activity of CNS depressants related to hydrophobicity. Nature 1974; 252:52–4
28. Peoples RW, Ren H: Inhibition of N-methyl-D-aspartate receptors by straight-chain diols: Implications for the mechanism of the alcohol cutoff effect. Mol Pharmacol 2002; 61:169–76
29. Jurd R, Arras M, Lambert S, Drexler B, Siegwart R, Crestani F, Zaugg M, Vogt KE, Ledermann B, Antkowiak B, Rudolph U: General anesthetic actions *in vivo* strongly attenuated by a point mutation in the GABA(A) receptor beta3 subunit. FASEB J 2003; 17:250–2
30. Stewart DS, Pierce DW, Hotta M, Stern AT, Forman SA: Mutations at beta N265 in γ-aminobutyric acid type A receptors alter both binding affinity and efficacy of potent anesthetics. PLoS One 2014; 9:e111470
31. Desai R, Ruesch D, Forman SA: Gamma-amino butyric acid type A receptor mutations at beta2N265 alter etomidate efficacy while preserving basal and agonist-dependent activity. Anesthesiology 2009; 111:774–84
32. Gregoret LM, Rader SD, Fletterick RJ, Cohen FE: Hydrogen bonds involving sulfur atoms in proteins. Proteins 1991; 9:99–107
33. Bertaccini EJ, Yoluk O, Lindahl ER, Trudell JR: Assessment of homology templates and an anesthetic binding site within the γ-aminobutyric acid receptor. Anesthesiology 2013; 119:1087–95
34. Franks NP: Structural comparisons of ligand-gated ion channels in open, closed, and desensitized states identify a novel propofol-binding site on mammalian γ-aminobutyric acid type A receptors. Anesthesiology 2015; 122:787–94
35. Bu W, Pereira LM, Eckenhoff RG, Yuki K: Stereoselectivity of isoflurane in adhesion molecule leukocyte function-associated antigen-1. PLoS One 2014; 9:e96649
36. Shanmugasundararaj S, Zhou X, Neunzig J, Bernhardt R, Cotten JF, Ge R, Miller KW, Raines DE: Carboetomidate: An analog of etomidate that interacts weakly with 11β-hydroxylase. Anesth Analg 2013; 116:1249–56
37. Sear JW: What makes a molecule an anaesthetic? Studies on the mechanisms of anaesthesia using a physicochemical approach. Br J Anaesth 2009; 103:50–60
38. Sewell JC, Sear JW: Derivation of preliminary three-dimensional pharmacophoric maps for chemically diverse intravenous general anaesthetics. Br J Anaesth 2004; 92:45–53
39. Sewell JC, Raines DE, Eger EI II, Laster MJ, Sear JW: A comparison of the molecular bases for N-methyl-D-aspartate-receptor inhibition *versus* immobilizing activities of volatile aromatic anesthetics. Anesth Analg 2009; 108:168–75